

Characterization of Gemstones Using Nanoparticle Enhanced Laser Induced Breakdown Spectroscopy (NELIBS)

Eng Wei Hang¹, Syed Zuhaib Haider Rizvi^{1*}

¹ Department of Physics and Chemistry, Universiti Tun Hussein Onn Malaysia Kampus Cawangan Pagoh, Hab Pendidikan Tinggi Pagoh, KM 1, Jalan Panchor, 84600 Pagoh, Muar, Johor, MALAYSIA.

*Corresponding Author: syedzuhaib@uthm.edu.my

DOI: <https://doi.org/10.30880/ekst.2024.04.01.032>

Article Info

Received: 27 December 2023

Accepted: 13 June 2024

Available online: 27 July 2024

Keywords

LIBS, NELIBS, Gemstones

Abstract

Gemstone characterization is an important aspect of gemology and requires precise analytical techniques. Laser-Induced Breakdown Spectroscopy (LIBS) has shown its ability to analyse multiple elements rapidly with a single shot of laser using atomic emission principles. However, Laser-Induced Breakdown Spectroscopy (LIBS) has its own drawback in characterizing gemstones due to their high refractive index, causing inefficient ablation, crack formation, and limitations in detecting trace elements and complex compounds. This research is mainly aimed to enhance the signal of emission spectrum as well as compare the damage induced by Nanoparticle Enhanced Laser Induced Breakdown Spectroscopy (NELIBS). This study involved the deposition of gold (Au NPs) nanoparticles onto samples of Blue Sapphire and Opal gemstones using a micropipette and analysing them with LIBS using a pulsed Nd:YAG laser and HR4000+ spectrometer with the help of Spectrasuite software. The research conducted has demonstrates the enhancement of the laser energy absorption on the sample. For instance, this research has shown that NELIBS significantly enhanced the intensity of aluminium's emission spectra around 11 times in blue sapphire compared to the conventional LIBS experiment. This enhancement can be explained by an increase in signal intensity as well as the enhanced spectral emissions. NELIBS has demonstrated its ability to prevent direct interaction between intense laser pulses and gemstones, thus reducing the laser-induced damage to the sample. This also leads to enhanced plasma formation and radiation emission, thereby enhancing the accuracy and sensitivity for gemstone analysis.

1. Introduction

Gemstone characterization is an essential aspect of gemology, requiring the implementation of accurate analytical techniques. Precious gemstones, which are renowned for their scarcity, aesthetic appeal, and resilience, are frequently formed by natural processes at depths exceeding hundreds of thousands of feet beneath the Earth's surface [1]. The objective of this study is to provide an in-depth characterization of gemstones using the Nanoparticle-Enhanced Laser-Induced Breakdown Spectroscopy (NELIBS) technique. Considered highly valued for its ability to collect data covering a wide spectral range using a single laser pulse, the Laser-Induced Breakdown Spectroscopy (LIBS) method is extensively utilized in gemstone analysis. This data is then analysed to identify the emission spectral lines of various elements present in the gemstone. However, despite its usefulness

in gemology characterization, LIBS technique does have certain limitations. The aforementioned issues arise due to the semi-transparent characteristics of gemstones, resulting in insufficient ablation, the formation of cracks, and constraints in the detection of trace elements and complex compounds. In contrast, alternative techniques such as X-Ray Diffraction (XRD) and Scanning Electron Microscopy (SEM) are also effective but are characterized by longer processing times and the need for sophisticated and costly equipment, while the LIBS technique has been recognized as a faster and more straightforward approach for conducting on-site and in situ investigations [2]. The main goal of this study was to develop the NELIBS experimental setup and then analyse and compare the LIBS and NELIBS spectra to examine the signal enhancement and potential laser-induced damage on gemstone surfaces caused by NELIBS and conventional LIBS techniques.

In order to address the constraints associated with LIBS, the NELIBS technique involves the deposition of metallic nanoparticles onto the surface of the gemstone. The presence of these nanoparticles prevents direct interaction between the sample and the pulsed laser, resulting in a localized amplification of the electromagnetic field surrounding the surface of the sample and the metallic nanoparticles. The introduction of metallic nanoparticles leads to enhanced energy absorption, thereby enhancing plasma formation and facilitating the identification of the emission spectrum [3].

This paper provides a comprehensive overview of the methodology employed in the NELIBS experimental setup. It includes detailed information on the alignment and positioning of LIBS components, the experimental procedures followed, the preparation of samples, and the results obtained from the analysis of emission spectral lines. The study focuses specifically on the characterization of gemstones using both LIBS and NELIBS techniques. The main objective of this study is to observe the enhancement of the intensity of emission spectrum and evaluate the potential damage of NELIBS and LIBS on the integrity of the samples.

The study's significance lies in its establishment of a benchmark for future research in gemstone characterization using the NELIBS technique. This paper presents a comprehensive analysis of the obtained results, highlighting the potential of NELIBS to advance gemological studies. The NELIBS technique shows a significant enhancement in emission spectral lines while efficiently reducing the potential of laser-induced damage. In this study, some recommendations for optimizing NELIBS in gemology were also presented.

2. Materials and Methods

This section provides a comprehensive overview of the materials and methods used in this study, collectively referred to as the methodology, in order to ensure the successful execution of the research. The experimental setups and alignments in NELIBS were meticulously designed and recorded using detailed flowcharts that outline each step of the procedure, beginning with the initial sample preparation and concluding with the completion of the experiment.

2.1 Materials: Sample Preparation

The experimental samples used in this study are Opal ($\text{SiO}_2 \cdot n\text{H}_2\text{O}$) and Blue Sapphire (Al_2O_3), as depicted in Fig. 1. In regard to the metallic nanoparticle selection, a colloidal solution of gold nanoparticles (AuNPs) procured from Sigma Aldrich was employed for NELIBS experiments. The measurement of the AuNPs' size is estimated to be around 20nm, while their concentration is approximately 6.54×10^{11} particles/mL. Using an adjustable micropipette with a volume range of 0.5 μL to 10 μL , two layers of 1 drop of 2 μL AuNPs were deposited onto the surface of the sample during the sample preparation stage in preparation for subsequent NELIBS experiments. Prior to drying, a 2 μL drop of AuNPs was deposited onto the surface of the sample and allowed to remain until a visible layer formed. After deposition of the second layer of a 2 μL drop of AuNPs onto the surface of the sample, the sample was allowed to dry once more. Then, the sample preparation is considered complete.



Fig. 1 Gemstones (a) Blue Sapphire (Al_2O_3); (b) Opal ($\text{SiO}_2 \cdot n\text{H}_2\text{O}$)

2.2 Methods: NELIBS Experimental Procedure

A flowchart for NELIBS and LIBS is illustrated in Fig. 2. Firstly, the NELIBS and LIBS experiment was set up. After that, 2 layers of 1 drop of 2 μL of gold nanoparticles colloidal solution (AuNPs) were deposited onto the sample surface using an adjustable micropipette. The first layer of 1 drop of 2 μL of AuNPs was deposited and allowed to dry until a visible layer formed, then the second layer was deposited in a similar way. A visible stain layer formed on the surface of sample after the sample preparation is completed. Gemstones with nanoparticles layers were placed on a sample holder.

After the experimental setup and sample preparation were completed, the Nd:YAG laser system was set to 1064nm of wavelength, 50mJ/pulse of laser energy, 10mm of laser beam spot size, and 1Hz of repetition rate, and then activated. The laser beam emitted from the Nd:YAG laser head gun was directed through the planoconvex lens and focused onto the sample surface to a spot size of 1.8 mm in diameter. This resulted in laser-matter interaction as well as plasma formation.

During the plasma formation, the emitted photon from the plasma was then guided via an end of the fibre optic cable to its optimal position, where the optimised distance is approximately 20mm and an angle of 35 degrees to the sample surface. While another end of the fibre optic cable is connected to the spectrometer, the collected photons or light are transmitted into the spectrometer and then experience light dispersion inside the spectrometer mechanism. The dispersed lights as optical signals were then converted into electrical signals by using the SpectraSuite software. Thus, the emission spectral lines were obtained.

If, for any reason, the intensity of the emission spectrum signal was too weak or contained too much background noise and it could not be identified against the National Institute of Standards and Technology (NIST) Atomic Spectral Database, every step from the stage of sample preparation was repeated until the emission spectral lines were sufficient enough to identify the elements that contains in the sample. Subsequently, all the spectrum data were recorded and analysed. The experiment was repeated for both LIBS and NELIBS, as well as different gemstone samples.

After the LIBS and NELIBS experiments were completed, the samples were wiped down to ensure they were clean from contamination. The sample was then placed on the microscope stage. The focal length of the microscope lens was adjusted until the optical microscope image of the sample was clear and sharp enough to observe and analyse. Subsequently, all the optical microscope images of the samples were recorded.

2.3 Experimental Setup

Each component was arranged and aligned in the manner depicted in Fig. 3. A 50mm focal length planoconvex lens was oriented in accordance with the direction of the laser beam in order to concentrate the beam on the surface of the sample. In order to minimise surface damage, the distance between the laser and the sample was modified to around 35mm. This adjustment was made due to the fact that the laser beam would concentrate 15mm beyond the sample surface, producing a spot size of approximately 1.8mm. This parameter was optimised in order to reduce the breakdown of the sample surface. In addition, the larger the spot size obtained by adjusting the distance between the lens to the sample surface, the larger the interaction areas between the laser and nanoparticles, which will enhance the effectiveness of plasma formation.

The experiment utilised a Nd:YAG pulsed laser system as the source of the laser source. The laser was adjusted to a wavelength of 1064nm, an energy of 50mJ per pulse, a beam size of 10mm, and a repetition rate of 1Hz. The operated wavelength of the laser and the laser energy are limited due to the limitations of the instrument. The laser beam size of 10mm was also optimised in order to ensure the area of the nanoparticles will be effectively ablated. Vertical alignment and precise positioning of the Nd:YAG laser source with the planoconvex lens guarantee that the laser beam is centred on the planoconvex lens. To further guarantee an accurate laser beam focusing on the surface of the sample, the sample stage is positioned beneath the centre of the planoconvex lens.

By analysing the clarity of emission spectral lines with the SpectraSuite software, the optimal parameters for the position of the fibre optic cable were determined. A fibre optic cable end was firmly affixed and positioned at an optimal distance of 20mm and an angle of 35 degrees in order to transmit the light or photons produced during the plasma formation in an efficient manner. The position of fibre optic cable was optimised in order to maximise the efficient guidance of light into the fibre since this is an experiment based atomic emission spectroscopy. An alternative ending of the fibre optic cable was utilised to connect the spectrometer, a Toshiba CCD camera, to the Ocean Optics HR4000 spectrometer with a resolution of 0.3nm. The laser source was synchronised with the spectroscopic system through the utilisation of a pulse generator (Stanford DG 535). The light that was emitted underwent dispersion within the spectroscopic system via its prism and grating before being transmitted to the CCD camera. Following their conversion to electrical signals, the acquired optical signals underwent additional processing utilising the SpectraSuite software. The analysis and recording of the emission spectral lines of the samples were accomplished with the assistance of SpectraSuite software. The identification of the elements present in the samples' composition was accomplished through the utilisation of the NIST Atomic Spectral Database as well as the observation and analysis of emission spectral lines.

Furthermore, to further examine the potential surface damage caused by LIBS and NELIBS, optical microscope images of the samples were captured using an Olympus Opto-Digital Microscope System after the LIBS and NELIBS experiments.

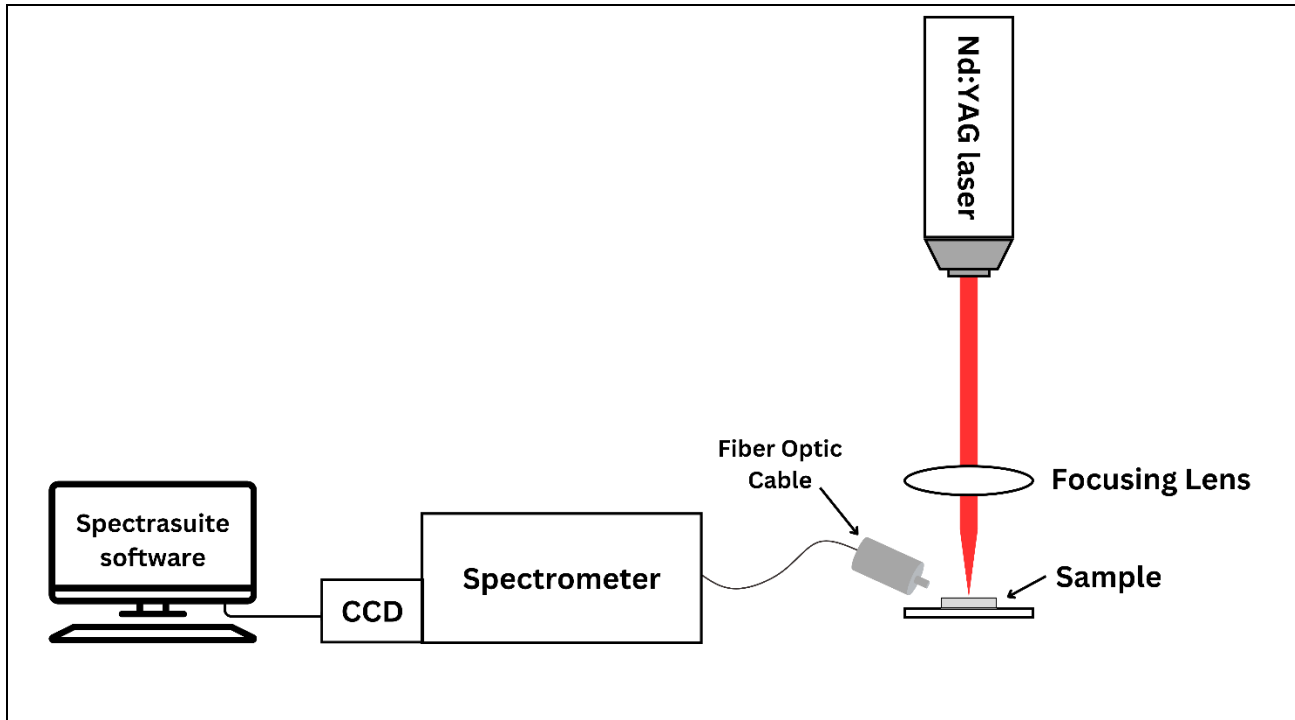


Fig. 2 Schematic diagram of LIBS and NELIBS experimental setup

3. Results and Discussion

This chapter delves into the elemental identification of gemstones, focusing on signal enhancement and damage induced by both LIBS and NELIBS techniques.

3.1 Elemental Identification

The NELIBS technique was used to analyse the chemical composition of blue sapphire and opal gemstones, and to identify any additional elements present. The chemical composition of blue sapphire is chemically named Al_2O_3 . A significant enhancement over the conventional LIBS technique was observed in the detection of aluminium at specific wavelengths of 394.38nm and 396.13nm in blue sapphire. Despite a peak overlap at 394.38nm and 393.59nm, the utilisation of nanoparticles enhanced the sensitivity of the detection system. Additional significant enhancement was observed in the detection of oxygen, the second primary element of a blue sapphire gemstone, at a particular wavelength of 777.35nm. In addition, NELIBS detection and enhancement were observed for additional elements present in blue sapphire, including barium, calcium, sodium, and potassium.

In contrast, silicon was effectively identified at wavelengths of 251.58nm and 288.14nm in opal gemstone, which is chemically represented as $\text{SiO}_2 \cdot n\text{H}_2\text{O}$; this represents a significant improvement over conventional LIBS. Oxygen and hydrogen, two additional primary elements found in opal gemstones, were detected at wavelengths of 777.35nm and 656.26nm, respectively. Furthermore, the first ionization level for oxygen was detected at wavelengths of 431.86nm and 464.88nm, whereas the first ionization level for silicon was detected at 634.71nm and 637.16nm. Furthermore, the NELIBS technique effectively detected and enhanced the signal of other elements, including strontium, potassium, sodium, and calcium.

NELIBS has the capability to detect a wide variety of elements present in a sample. Any elements detected beyond the chemical composition of the gemstone can be classified and described as impurities or contaminants. As a consequence of airborne particles and environmental pollutants, surface contaminants that may gradually accumulate on gemstones. Lint-free tissue paper and isopropyl alcohol have the potential to expose contamination to the surface of the sample. In addition, impurities may have been present in gemstones by nature during their formation.

The incorporation of nanoparticles into the LIBS technique resulted in a notable improvement in the emission spectral lines observed from blue sapphire and opal. The observed enhancement can be attributed to the

generation of localized surface plasmon resonance (SPR) by nanoparticles, resulting in an enhanced electromagnetic field around the surface of the sample [4]. As a result, this phenomenon indirectly enhances the emission of spectral lines during the interaction between the laser and the sample.

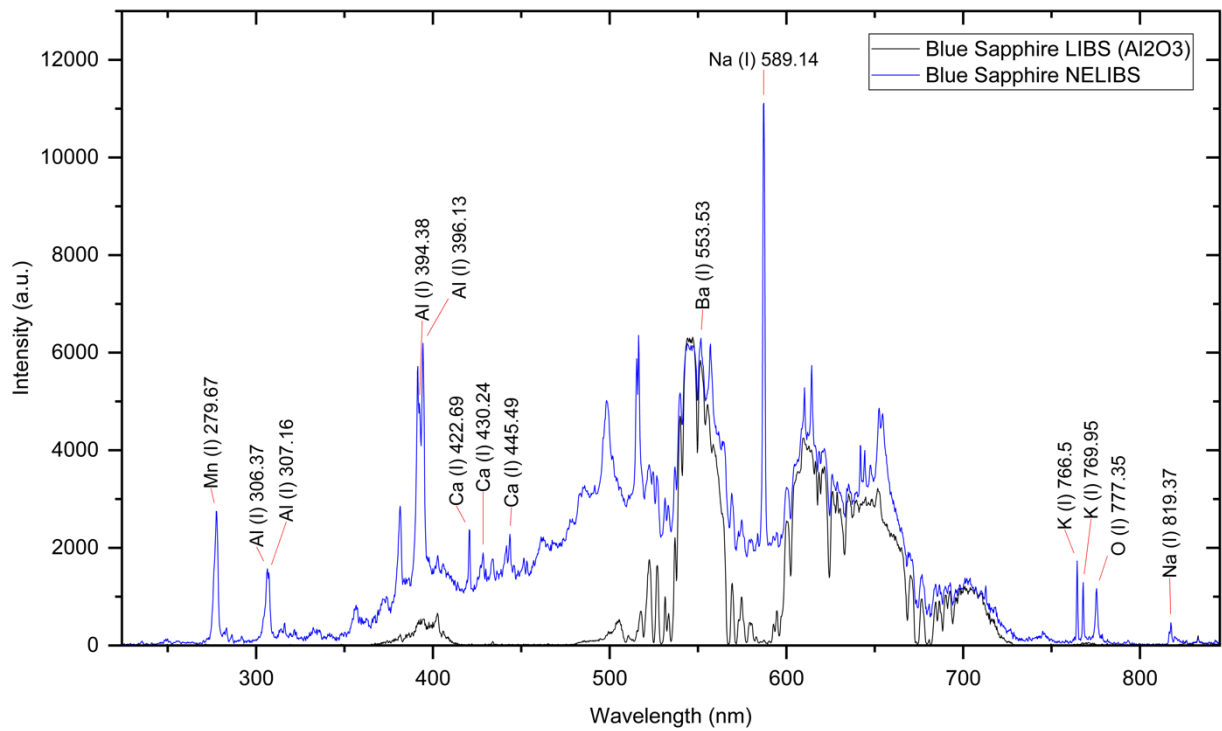


Fig. 3 LIBS and NELIBS spectra of Blue Sapphire (Al_2O_3) with identified elemental lines

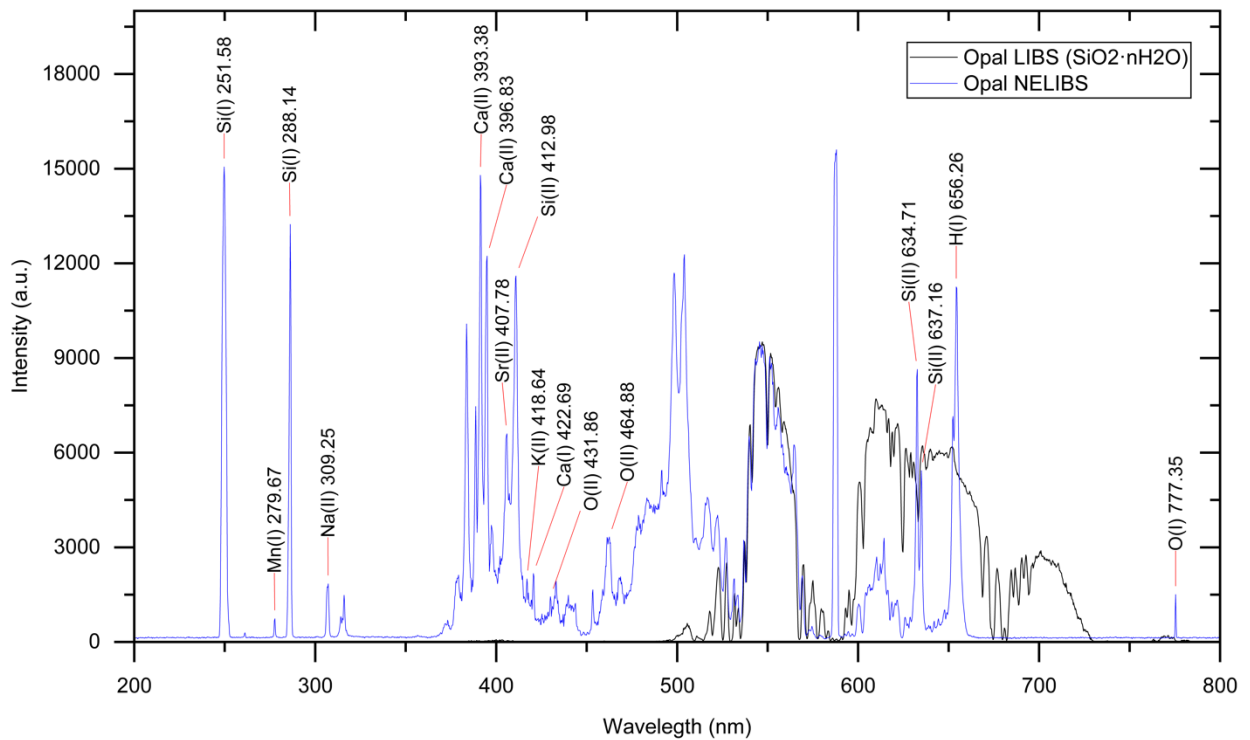


Fig. 4 LIBS and NELIBS spectra of Opal ($SiO_2 \cdot nH_2O$) with identified elemental lines

3.2 Signal Enhancement

The effectiveness of the NELIBS technique in enhancing the signal of emission spectral lines has been proved through a comparative analysis of the results obtained from the LIBS and NELIBS experiments. The Al spectral lines from the blue sapphire gemstone are depicted in Fig. 6 using the NELIBS technique. The red lines represented the emission spectral lines of the blue sapphire gemstone using the NELIBS technique, while the black lines represented the emission spectral lines of the blue sapphire using the conventional LIBS technique. The NELIBS signal of aluminium for blue sapphire has been substantially amplified by approximately 11 times over the conventional LIBS signal, whereas the NELIBS signal of oxygen shows even greater enhancement as was non existing in conventional LIBS spectrum.

In Fig. 7, the red lines represent the emission spectral lines of the opal gemstone using the NELIBS technique, contrasting with the black lines representing the emission spectral lines of the opal gemstone using conventional LIBS. The LIBS emission spectral lines of opal within the wavelength range from 200nm to 500nm were unidentifiable. However, NELIBS successfully enhanced the signal, allowing for the detection of silicon and oxygen. Overall, NELIBS significantly enhanced the signal of emission spectral lines for both blue sapphire and opal gemstones, within the wavelength range of 350nm to 530nm and 250nm to 520nm, respectively.

The observed enhancement is attributed to the use of nanoparticles, which introduce the phenomenon of localized surface plasmon resonance (LSPR). A significant enhancement in the electromagnetic field near the surface of the nanoparticles takes place when the frequency of the incident light coincides with the inherent frequency of the conduction electrons [5]. Concurrently, this substantial enhancement of the electromagnetic field enables more electron emissions [6][7]. In addition, the electromagnetic field in the vicinity of the sample is amplified by the resonant oscillations of the conduction electrons induced by the laser [8]. This effect results in higher excitation temperature and emitter density during laser-matter interaction, which ultimately amplifies the signal of the emission spectrum [9]. In addition, plasmonic coupling enhances the energy of the incident laser, given that nanoparticles can reduce the sample breakdown threshold and induce sample breakdown with better efficiency [10,11].

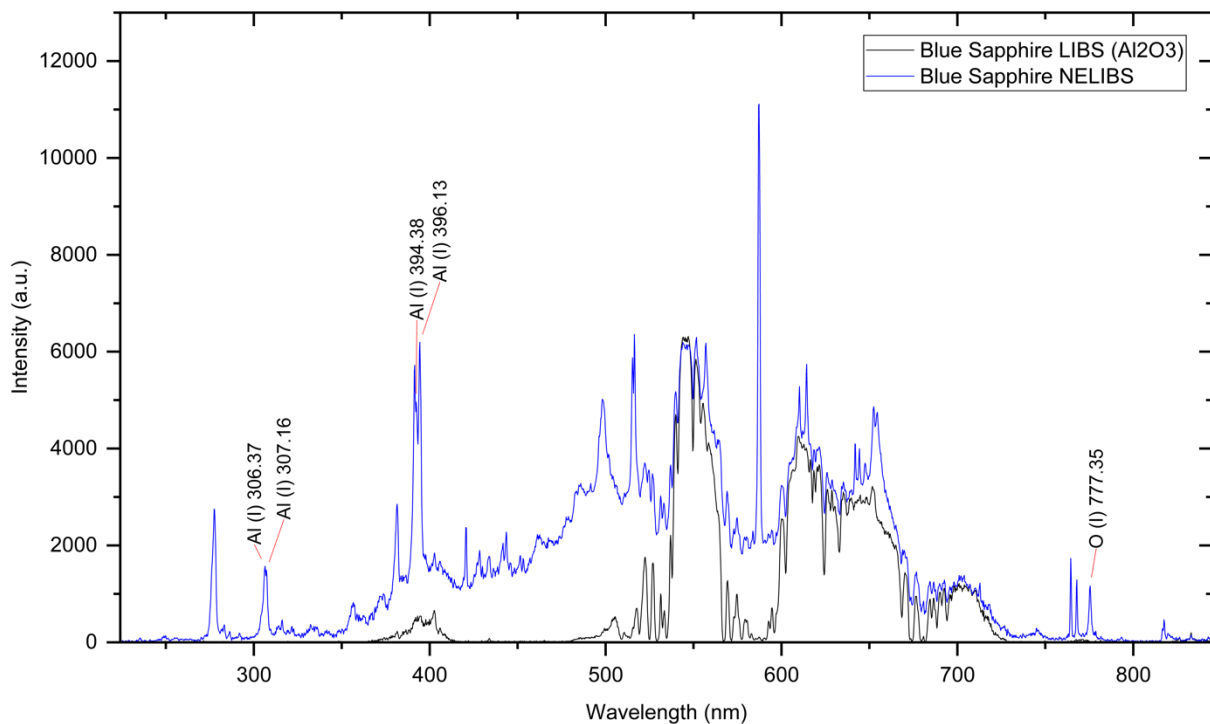


Fig. 5 Emission spectral lines of chemical composition elements in blue sapphire (Al_2O_3)

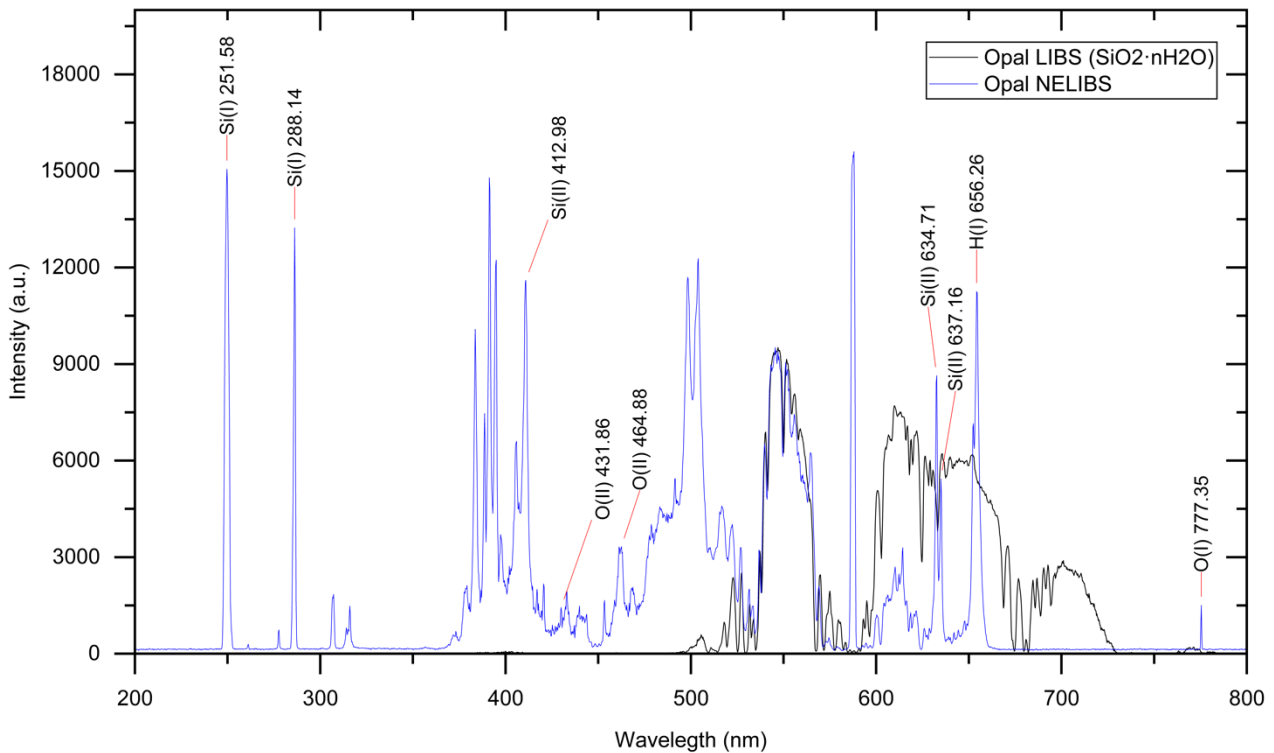


Fig. 6 Emission spectral lines of chemical composition elements in Opal ($\text{SiO}_2 \cdot n\text{H}_2\text{O}$)

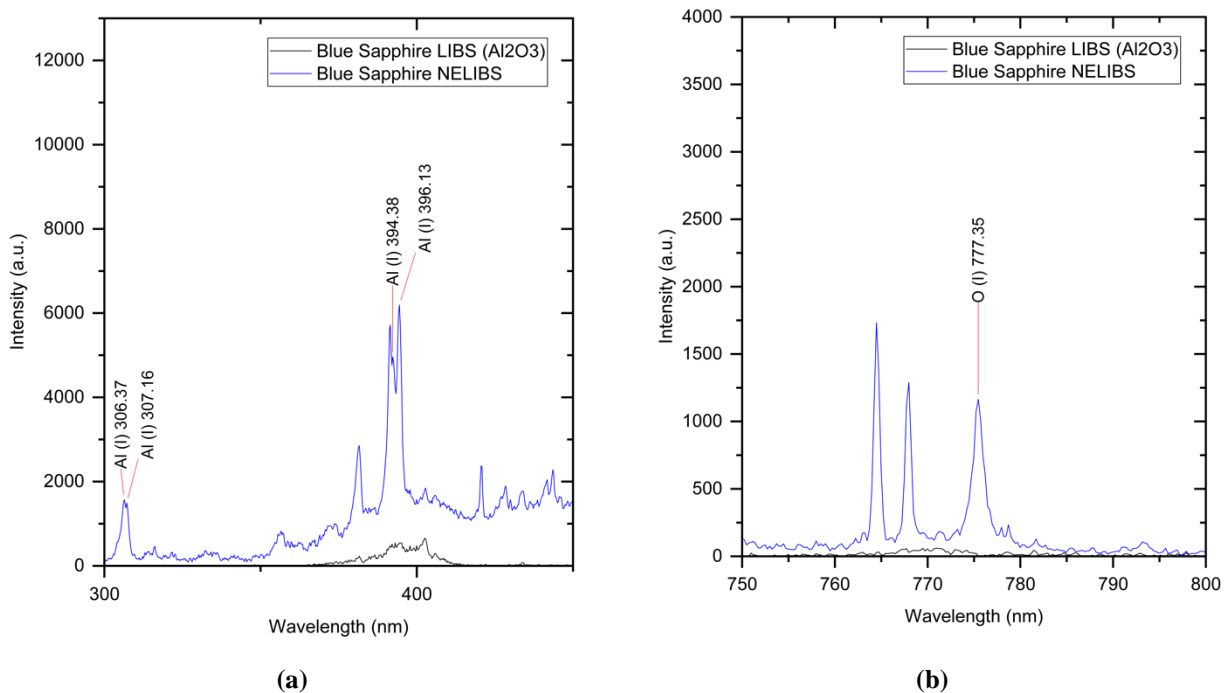


Fig. 7 Emission spectral lines of (a) aluminium; (b) oxygen in blue sapphire (Al_2O_3)

3.3 Damage Induced

The LIBS has consistently faced challenges, especially when implemented on semi-transparent substances such as gemstones. This concern stems from the ability of the focused laser discharge to penetrate the sample, causing cracks and craters that subsequently affect the gemstones' intrinsic value. In this study, the Olympus Opto-Digital

Microscope System has been used in order to further investigate and observe the damage that was caused by laser in LIBS and NELIBS experiments. The study's findings indicate that the NELIBS technique effectively reduced the negative impact of the focused laser to the sample, while simultaneously improving the emission intensity of spectral lines. The comparison of the damage caused by the focused laser in LIBS and NELIBS experiments on blue sapphire and opal gemstones is depicted in the microscopic images in Fig. 8. The damage induced by the focused laser utilizing the NELIBS is indicated with the red circle, while the damage induced by the focused laser by the conventional LIBS is indicated with the black circle in Fig. 8. In this study, it was observed that NELIBS significantly reduces the damage induced by the focused laser on semi-transparent substances, including opal gemstones and blue sapphire.

Through analysis of the interaction dynamics of the incoming laser pulse, the observed result can be clarified. In contrast to the direct interaction with the sample surface observed in LIBS experiments, the laser initially interacts with the layers of nanoparticles deposited on the surface of the sample. The nanoparticles induce the Localized Surface Plasmon Resonance (LSPR) as well as enhancing the electromagnetic field around the nanoparticle surface. Moreover, defects that are thermally insulated are introduced by nanoparticles, which function as localized heat sinks. Consequently, the nanoparticles absorb the laser energy, thereby reducing thermal damage to the gemstone, which may otherwise result in the formation of cracks or cavities in the sample [8]. Fundamentally, most of the incident laser energy is absorbed by nanoparticles, whereas localized heat sinks enhance the ionization processes and reduce the sample material's threshold breakdown, thereby decreasing the required threshold energy [4]. Ensuring this is of utmost importance to prevent the damage of gemstones, which becomes brittle or discoloured when exposed to high temperatures [12, 13]. In short, NELIBS demonstrates its capacity to substantially reduce the damage induced by the focused laser on opal and blue sapphire gemstones.

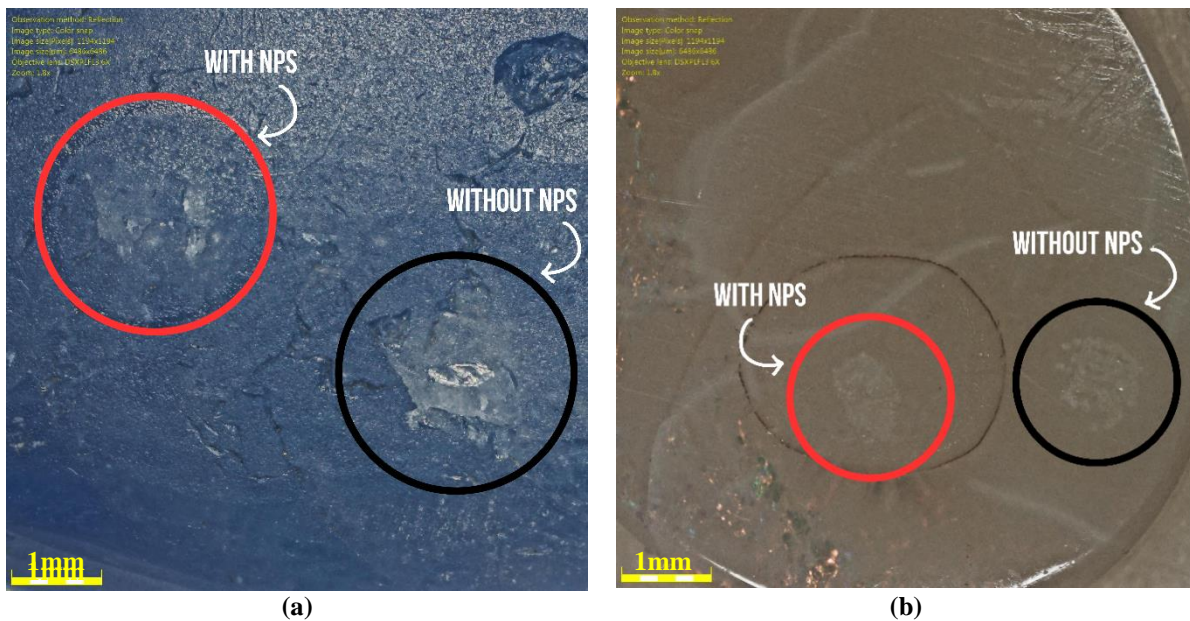


Fig. 8 Microscopic images of damage induced by focused laser on (a) Blue Sapphire (Al_2O_3); (b) Opal ($SiO_2 \cdot nH_2O$)

4. Conclusion

In general, NELIBS is an experimental method that, in its simplest form, decreases the likelihood of laser-induced damage while simultaneously enhancing the intensity of spectral lines. For instance, the NELIBS signal of aluminium for blue sapphire was enhanced approximately 11 times over the conventional LIBS signal at the specific wavelengths of 394.38nm and 396.13nm. This is achieved by employing gold nanoparticle deposition during the sample preparation step. It has been demonstrated that the nanoparticles may enhance plasma formation by the phenomenon referred to as Localized Surface Plasmon Resonance (LSPR). Consequently, this results in higher excitation temperatures and a more intense process of ionization.

In conclusion, the NELIBS technique has demonstrated remarkable effectiveness, through the utilization of nanoparticles, in reducing laser-induced damage and enhancing the signal of the emission spectrum. It is important to acknowledge that this research possesses certain constraints, and there exist possibilities for its enhancement. For instance, the experimental parameters could be enhanced through the manipulation of the time grating of the spectrometer or the utilization of a higher resolution spectrometer. It can enable the detection of emission spectral lines that are more intricate and refined.

Acknowledgement

Communication of this research is made possible through monetary assistance by Universiti Tun Hussein Onn Malaysia and the UTHM Publisher's Office via Publication Fund E15216. The authors would also like to thank the Faculty of Applied Sciences and Technology, Pagoh Higher Education Hub, and Universiti Tun Hussein Onn Malaysia for the facilities provided.

Conflict of Interest

Authors declare that there is no conflict of interests regarding the publication of the paper.

Author Contribution

The authors confirm contribution to the paper as follows: **study conception and design, data collection, methodology, analysis and interpretation of results:** Eng Wei Hang and Syed Zuhaib Haider Rizvi. All authors reviewed the results and approved the final version of the manuscript.

References

- [1] Cartier, L. E. (2019). Gemstones and sustainable development: Perspectives and trends in mining, processing and trade of precious stones. *Extractive Industries and Society*, 6(4), 1013–1016. <https://doi.org/10.1016/j.exis.2019.09.005>
- [2] Khan, M. R., Haq, S. U., Abbas, Q., & Nadeem, A. (2022). Improvement in signal sensitivity and repeatability using copper nanoparticle-enhanced laser-induced breakdown spectroscopy. *Spectrochimica Acta - Part B Atomic Spectroscopy*, 195. <https://doi.org/10.1016/j.sab.2022.106507>
- [3] Poggialini, F., Campanella, B., Legnaioli, S., Pagnotta, S., & Palleschi, V. (2020). Investigating double pulse nanoparticle enhanced laser induced breakdown spectroscopy. *Spectrochimica Acta - Part B Atomic Spectroscopy*, 167. <https://doi.org/10.1016/j.sab.2020.105845>
- [4] De Giacomo, A., Gaudiuso, R., Koral, C., Dell'Aglio, M., & De Pascale, O. (2013). Nanoparticle-enhanced laser-induced breakdown spectroscopy of metallic samples. *Analytical Chemistry*, 85(21), 10180–10187. <https://doi.org/10.1021/ac4016165>
- [5] Dell'Aglio, M., Salajková, Z., Mallardi, A., Sportelli, M. C., Kaiser, J., Cioffi, N., & De Giacomo, A. (2021). Sensing nanoparticle-protein corona using nanoparticle enhanced Laser Induced Breakdown Spectroscopy signal enhancement. *Talanta*, 235. <https://doi.org/10.1016/j.talanta.2021.122741>
- [6] Abdelhamid, M., Attia, Y. A., & Abdel-Harith, M. (2020). The significance of nano-shapes in nanoparticle-enhanced laser-induced breakdown spectroscopy. *Journal of Analytical Atomic Spectrometry*, 35(12), 2982–2989. <https://doi.org/10.1039/d0ja00329h>
- [7] Dell'Aglio, M., Alrifai, R., & De Giacomo, A. (2018). Nanoparticle Enhanced Laser Induced Breakdown Spectroscopy (NELIBS), a first review. In *Spectrochimica Acta - Part B Atomic Spectroscopy* (Vol. 148, pp. 105–112). Elsevier B.V. <https://doi.org/10.1016/j.sab.2018.06.008>
- [8] Koral, C., Dell'Aglio, M., Gaudiuso, R., Alrifai, R., Torelli, M., & De Giacomo, A. (2018). Nanoparticle-Enhanced Laser Induced Breakdown Spectroscopy for the noninvasive analysis of transparent samples and gemstones. *Talanta*, 182, 253–258. <https://doi.org/10.1016/j.talanta.2018.02.001>
- [9] Koral, C., De Giacomo, A., Mao, X., Zorba, V., & Russo, R. E. (2016). *Nanoparticle Enhanced Laser Induced Breakdown Spectroscopy for Improving the Detection of Molecular Bands*. <https://www.elsevier.com/open-access/userlicense/1.0/>
- [10] Abidin, N. A. Z. (2021). Development of high iron and high energy snack bar: nutritional content analysis and sensory evaluation. *Enhanced Knowledge in Sciences and Technology*, 1(2), 201-207.
- [11] De Giacomo, A., Alrifai, R., Gardette, V., Salajková, Z., & Dell'Aglio, M. (2020). Nanoparticle enhanced laser ablation and consequent effects on laser induced plasma optical emission. *Spectrochimica Acta - Part B Atomic Spectroscopy*, 166. <https://doi.org/10.1016/j.sab.2020.105794>
- [12] De Giacomo, A., Gaudiuso, R., Koral, C., Dell'Aglio, M., & De Pascale, O. (2014). Nanoparticle Enhanced Laser Induced Breakdown Spectroscopy: Effect of nanoparticles deposited on sample surface on laser ablation and plasma emission. *Spectrochimica Acta - Part B Atomic Spectroscopy*, 98, 19–27. <https://doi.org/10.1016/j.sab.2014.05.010>
- [13] Yunus, Z. M., & Azaha, N. A. N. (2021). Jackfruit Seeds Starch-Based Coagulant for Synthetic Textile Wastewater Remediation. *Enhanced Knowledge in Sciences and Technology*, 1(2), 72-80.